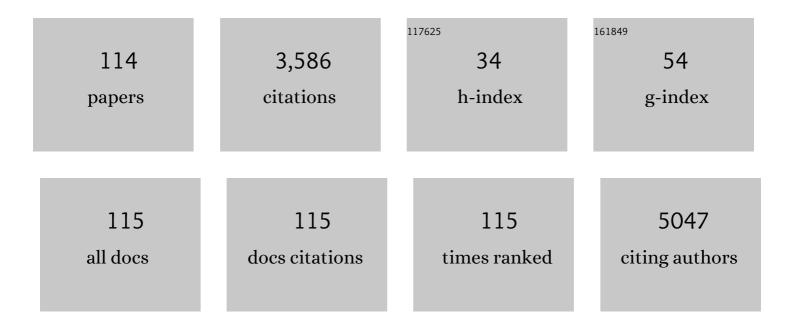
Sayan Bhattacharyya

List of Publications by Year in descending order

Source: https://exaly.com/author-pdf/1473275/publications.pdf Version: 2024-02-01



#	Article	IF	CITATIONS
1	Porous NiFe-Oxide Nanocubes as Bifunctional Electrocatalysts for Efficient Water-Splitting. ACS Applied Materials & Interfaces, 2017, 9, 41906-41915.	8.0	229
2	Multifunctional carbon-nanotube cellular endoscopes. Nature Nanotechnology, 2011, 6, 57-64.	31.5	214
3	Value added transformation of ubiquitous substrates into highly efficient and flexible electrodes for water splitting. Nature Communications, 2018, 9, 2014.	12.8	126
4	A template-free, sonochemical route to porous ZnO nano-disks. Microporous and Mesoporous Materials, 2008, 110, 553-559.	4.4	113
5	Iron Nitride Family at Reduced Dimensions: A Review of Their Synthesis Protocols and Structural and Magnetic Properties. Journal of Physical Chemistry C, 2015, 119, 1601-1622.	3.1	110
6	Microwave-Assisted Insertion of Silver Nanoparticles into 3-D Mesoporous Zinc Oxide Nanocomposites and Nanorods. Journal of Physical Chemistry C, 2008, 112, 659-665.	3.1	89
7	Limiting Heterovalent B-Site Doping in CsPbl ₃ Nanocrystals: Phase and Optical Stability. ACS Energy Letters, 2019, 4, 1364-1369.	17.4	86
8	Lead free double perovskite oxides Ln 2 NiMnO 6 (Ln = La, Eu, Dy, Lu), a new promising material for photovoltaic application. Materials Science and Engineering B: Solid-State Materials for Advanced Technology, 2017, 226, 10-17.	3.5	82
9	Dependence of halide composition on the stability of highly efficient all-inorganic cesium lead halide perovskite quantum dot solar cells. Solar Energy Materials and Solar Cells, 2018, 185, 28-35.	6.2	82
10	Copper Azide Confined Inside Templated Carbon Nanotubes. Advanced Functional Materials, 2010, 20, 3168-3174.	14.9	73
11	Enhanced Low-Field Magnetoresistance in La _{0.71} Sr _{0.29} MnO ₃ Nanoparticles Synthesized by the Nonaqueous Sol–Gel Route. Chemistry of Materials, 2014, 26, 1702-1710.	6.7	70
12	Small diameter carbon nanopipettes. Nanotechnology, 2010, 21, 015304.	2.6	69
13	Bimetallic nanoparticle decorated perovskite oxide for state-of-the-art trifunctional electrocatalysis. Journal of Materials Chemistry A, 2019, 7, 19453-19464.	10.3	68
14	Phenomenal Ultraviolet Photoresponsivity and Detectivity of Graphene Dots Immobilized on Zinc Oxide Nanorods. ACS Applied Materials & Interfaces, 2016, 8, 35496-35504.	8.0	60
15	Graphitic porous carbon derived from human hair as â€~green' counter electrode in quantum dot sensitized solar cells. Carbon, 2016, 107, 395-404.	10.3	60
16	High performance duckweed-derived carbon support to anchor NiFe electrocatalysts for efficient solar energy driven water splitting. Journal of Materials Chemistry A, 2018, 6, 18948-18959.	10.3	58
17	Dual Sensitization Strategy for High-Performance Core/Shell/ <i>Quasi-shell</i> Quantum Dot Solar Cells. Chemistry of Materials, 2015, 27, 4848-4859.	6.7	56
18	A microwave synthesized Cu _x S and graphene oxide nanoribbon composite as a highly efficient counter electrode for quantum dot sensitized solar cells. Nanoscale, 2016, 8, 10632-10641.	5.6	54

#	Article	IF	CITATIONS
19	Doping the Smallest Shannon Radii Transition Metal Ion Ni(II) for Stabilizing α-CsPbl ₃ Perovskite Nanocrystals. Journal of Physical Chemistry Letters, 2019, 10, 7916-7921.	4.6	53
20	Oxygenâ€Defectâ€Rich Cobalt Ferrite Nanoparticles for Practical Water Electrolysis with High Activity and Durability. ChemSusChem, 2020, 13, 3875-3886.	6.8	52
21	Tweaking Nickel with Minimal Silver in a Heterogeneous Alloy of Decahedral Geometry to Deliver Platinumâ€like Hydrogen Evolution Activity. Angewandte Chemie - International Edition, 2020, 59, 2881-2889.	13.8	50
22	Lemon grass derived porous carbon nanospheres functionalized for controlled and targeted drug delivery. Carbon, 2016, 100, 223-235.	10.3	45
23	Zinc-diffused silver indium selenide quantum dot sensitized solar cells with enhanced photoconversion efficiency. Journal of Materials Chemistry A, 2017, 5, 11746-11755.	10.3	43
24	All-inorganic quantum dot assisted enhanced charge extraction across the interfaces of bulk organo-halide perovskites for efficient and stable pin-hole free perovskite solar cells. Chemical Science, 2019, 10, 9530-9541.	7.4	43
25	Plight of Mn Doping in Colloidal CdS Quantum Dots To Boost the Efficiency of Solar Cells. Journal of Physical Chemistry C, 2015, 119, 13404-13412.	3.1	42
26	An earth-abundant bimetallic catalyst coated metallic nanowire grown electrode with platinum-like pH-universal hydrogen evolution activity at high current density. Chemical Science, 2020, 11, 3893-3902.	7.4	42
27	Molybdenum sulfide–reduced graphene oxide p–n heterojunction nanosheets with anchored oxygen generating manganese dioxide nanoparticles for enhanced photodynamic therapy. Chemical Science, 2018, 9, 8982-8989.	7.4	40
28	Surface Charge Modulation of Perovskite Oxides at the Crystalline Junction with Layered Double Hydroxide for a Durable Rechargeable Zinc–Air Battery. ACS Applied Materials & Interfaces, 2019, 11, 35853-35862.	8.0	40
29	Carbon dots with tunable concentrations of trapped anti-oxidant as an efficient metal-free catalyst for electrochemical water oxidation. Journal of Materials Chemistry A, 2016, 4, 14614-14624.	10.3	39
30	Photoactive Core–Shell Nanorods as Bifunctional Electrodes for Boosting the Performance of Quantum Dot Sensitized Solar Cells and Photoelectrochemical Cells. Chemistry of Materials, 2018, 30, 6071-6081.	6.7	39
31	Photocatalyzed borylation using water-soluble quantum dots. Chemical Communications, 2019, 55, 6201-6204.	4.1	38
32	A One-step, Template-free Synthesis, Characterization, Optical and Magnetic Properties of Zn _{1â^'<i>x</i>} Mn _{<i>x</i>} Te Nanosheets. Chemistry of Materials, 2009, 21, 326-335.	6.7	37
33	Efficient Dye Degradation Catalyzed by Manganese Oxide Nanoparticles and the Role of Cation Valence. ChemistrySelect, 2016, 1, 4265-4273.	1.5	37
34	One-pot fabrication and magnetic studies of Mn-doped TiO ₂ nanocrystals with an encapsulating carbon layer. Nanotechnology, 2008, 19, 495711.	2.6	35
35	Interface Engineering in Quantum-Dot-Sensitized Solar Cells. Langmuir, 2018, 34, 10197-10216.	3.5	34
36	Mössbauer and magnetic studies of MFe2O4(M = Co, Ni) nanoparticles. Hyperfine Interactions, 2007, 1 153-159.	165. 0.5	33

SAYAN BHATTACHARYYA

#	Article	IF	CITATIONS
37	Sonochemical Insertion of Silver Nanoparticles into Two-Dimensional Mesoporous Alumina. Journal of Physical Chemistry C, 2007, 111, 11161-11167.	3.1	32
38	Luminescent and Ferromagnetic CdS:Mn ²⁺ /C Coreâ^'Shell Nanocrystals. Journal of Physical Chemistry C, 2010, 114, 22002-22011.	3.1	32
39	Oneâ€Step Solventâ€Free Synthesis and Characterization of Zn _{1â^'x} Mn _x Se@C Nanorods and Nanowires. Advanced Functional Materials, 2008, 18, 1641-1653.	14.9	31
40	Enhanced catalytic activity of palladium nanoparticles confined inside porous carbon in methanol electro-oxidation. Green Chemistry, 2015, 17, 1572-1580.	9.0	31
41	Synthesis, Characterization, and Room-Temperature Ferromagnetism in Cobalt-Doped Zinc Oxide (ZnO:Co ²⁺) Nanocrystals Encapsulated in Carbon. Journal of Physical Chemistry C, 2008, 112, 4517-4523.	3.1	30
42	High Pressure Experimental Studies on CuO: Indication of Re-entrant Multiferroicity at Room Temperature. Scientific Reports, 2016, 6, 31610.	3.3	30
43	Localized Synthesis of Metal Nanoparticles Using Nanoscale Corona Discharge in Aqueous Solutions. Advanced Materials, 2009, 21, 4039-4044.	21.0	29
44	Maneuvering the Physical Properties and Spin States To Enhance the Activity of La–Sr–Co–Fe–O Perovskite Oxide Nanoparticles in Electrochemical Water Oxidation. ACS Applied Energy Materials, 2018, 1, 3342-3350.	5.1	29
45	One-Step Synthesis, Structural and Optical Characterization of Self-Assembled ZnO Nanoparticle Clusters with Quench-Induced Defects. Science of Advanced Materials, 2014, 6, 1160-1169.	0.7	29
46	Magnetic properties of ε-Fe3N–GaN core–shell nanowires. Nanotechnology, 2005, 16, 2012-2019.	2.6	28
47	One-Pot Synthesis and Characterization of Mn2+-Doped Wurtzite CdSe Nanocrystals Encapsulated with Carbon. Journal of Physical Chemistry C, 2008, 112, 7624-7630.	3.1	27
48	Mössbauer Studies of Nanosize CuFe2O4Particles. Hyperfine Interactions, 2004, 156/157, 57-61.	0.5	26
49	Highly Luminescent ZnxCd1â^'xSe/C Core/Shell Nanocrystals: Large Scale Synthesis, Structural and Cathodoluminescence Studies. ACS Nano, 2009, 3, 1864-1876.	14.6	24
50	Influence of the morphology of carbon nanostructures on the stimulated growth of gram plant. RSC Advances, 2016, 6, 43864-43873.	3.6	24
51	Enhancement of Magnetization through Interface Exchange Interactions of Confined NiO Nanoparticles within the Mesopores of CoFe ₂ O ₄ . Journal of Physical Chemistry C, 2016, 120, 5523-5533.	3.1	23
52	Shaping a Doped Perovskite Oxide with Measured Grain Boundary Defects to Catalyze Bifunctional Oxygen Activation for a Rechargeable Zn–Air Battery. ACS Applied Materials & Interfaces, 2020, 12, 40355-40363.	8.0	23
53	Magnetic Properties of Co and Ni Substituted É›-Fe3N Nanoparticles. Hyperfine Interactions, 2006, 164, 17-26.	0.5	22
54	Variation of magnetic ordering in Ĵµ-Fe3N nanoparticles. Chemical Physics Letters, 2010, 496, 122-127.	2.6	22

#	Article	IF	CITATIONS
55	Chemical Modifications of Porous Carbon Nanospheres Obtained from Ubiquitous Precursors for Targeted Drug Delivery and Live Cell Imaging. ACS Sustainable Chemistry and Engineering, 2018, 6, 8503-8514.	6.7	22
56	Spin-glass-like ordering in É>-Fe3â^'xNixN (0.1â‰ ¤ â‰ 0 .8) nanoparticles. Materials Chemistry and Physics, 2008, 108, 201-207.	4.0	21
57	Core/Shell Nanocrystal Tailored Carrier Dynamics in Hysteresisless Perovskite Solar Cells with â^1⁄420% Efficiency and Long Operational Stability. Journal of Physical Chemistry Letters, 2020, 11, 591-600.	4.6	21
58	Stacked Nanosheets of Pr1–xCaxMnO3 (x = 0.3 and 0.49): A Ferromagnetic Two-Dimensional Material with Spontaneous Exchange Bias. Journal of Physical Chemistry C, 2013, 117, 26351-26360.	3.1	19
59	Enhancing Multifunctionality through Secondary Phase Inclusion by Self-Assembly of Mn ₃ O ₄ Nanostructures with Superior Exchange Anisotropy and Oxygen Evolution Activity. Journal of Physical Chemistry C, 2017, 121, 25594-25602.	3.1	19
60	2D Heterojunction Between Double Perovskite Oxide Nanosheet and Layered Double Hydroxide to Promote Rechargeable Zincâ€Air Battery Performance. ChemElectroChem, 2020, 7, 5005-5012.	3.4	19
61	Photodetectors with High Responsivity by Thickness Tunable Mixed Halide Perovskite Nanosheets. ACS Applied Materials & Interfaces, 2021, 13, 43104-43114.	8.0	19
62	Heterovalent Substitution in Mixed Halide Perovskite Quantum Dots for Improved and Stable Photovoltaic Performance. Journal of Physical Chemistry C, 2021, 125, 5485-5493.	3.1	18
63	Thickness-Attuned CsPbBr ₃ Nanosheets with Enhanced <i>p</i> -Type Field Effect Mobility. Journal of Physical Chemistry Letters, 2021, 12, 1560-1566.	4.6	17
64	In Situ Cation Intercalation in the Interlayer of Tungsten Sulfide with Overlaying Layered Double Hydroxide in a 2D Heterostructure for Facile Electrochemical Redox Activity. Inorganic Chemistry, 2021, 60, 6911-6921.	4.0	17
65	Ferromagnetism in Lightly Doped Pr _{1–<i>x</i>} Ca _{<i>x</i>} MnO ₃ (<i>x</i> = 0.023, 0.036) Nanoparticles Synthesized by Microwave Irradiation. Chemistry of Materials, 2012, 24, 3758-3764.	6.7	16
66	Attuning the Electronic Properties of Two-Dimensional Co-Fe-O for Accelerating Water Electrolysis and Photolysis. ACS Applied Materials & amp; Interfaces, 2019, 11, 30682-30693.	8.0	16
67	Long Carrier Diffusion Length and Slow Hot Carrier Cooling in Thin Film Mixed Halide Perovskite. IEEE Journal of Photovoltaics, 2020, 10, 803-810.	2.5	16
68	Synthesis and characterization of É›-Fe3N/GaN, 54/46-composite nanowires. Materials Research Bulletin, 2008, 43, 272-283.	5.2	15
69	Cation Exchange in Zn–Ag–In–Se Core/Alloyed Shell Quantum Dots and Their Applications in Photovoltaics and Water Photolysis. Chemistry of Materials, 2019, 31, 161-170.	6.7	15
70	Charge transfer from perovskite oxide nanosheets to N-doped carbon nanotubes to promote enhanced performance of a zinc–air battery. Chemical Communications, 2020, 56, 8277-8280.	4.1	15
71	Magnetism of nanostructured iron nitride (Fe-N) systems. Physica Status Solidi C: Current Topics in Solid State Physics, 2004, 1, 3252-3259.	0.8	14
72	An electrochemically reversible lattice with redox active A-sites of double perovskite oxide nanosheets to reinforce oxygen electrocatalysis. Chemical Science, 2020, 11, 10180-10189.	7.4	14

#	Article	IF	CITATIONS
73	Magnetic interactions in ε-Fe3N–GaN nanocomposites. Journal of Applied Physics, 2007, 101, 113902.	2.5	13
74	Interplay of Porosity in γ-Al ₂ O ₃ -Doped ZnO Nanocomposites: A Comparative Study of Sonochemical and Microwave Reaction Routes. Journal of Physical Chemistry C, 2008, 112, 13156-13162.	3.1	13
75	Synthesis and magnetic characterization of CoMoN2 nanoparticles. Journal of Nanoparticle Research, 2010, 12, 1107-1116.	1.9	13
76	Cobalt Phosphide Nanorods with Controlled Aspect Ratios as Synergistic Photothermo-Chemotherapeutic Agents. ACS Applied Nano Materials, 2018, 1, 5237-5245.	5.0	13
77	Spin Disorder and Particle Size Effects in Cobalt Ferrite Nanoparticles with Unidirectional Anisotropy and Permanent Magnet-like Characteristics. Journal of Physical Chemistry C, 2020, 124, 25992-26000.	3.1	13
78	Electron Paramagnetic Resonance Spectroscopic Investigation of Manganese Doping in ZnL (L = O, S,) Tj ETQqO (0 0 rgBT /0	Overlock 10 T
79	Analysis of the acid, base and air oxidized carbon microspheres synthesized in a single step from waste engine oil. Corrosion Science, 2013, 73, 356-364.	6.6	12
80	Pressure-Induced Emergence of Visible Luminescence in Lead Free Halide Perovskite Cs ₃ Bi ₂ Br ₉ : Effect of Structural Distortion. Journal of Physical Chemistry C, 2021, 125, 3432-3440.	3.1	12
81	Ab Initio Study of the Structural, Electronic, Magnetic, and Hyperfine Properties of Ga _{<i>x</i>} Fe _{4–<i>x</i>} N (0.00 ≤i>x ≤.00) Nitrides. Journal of Physical Chemistry C, 2011, 115, 23081-23089.	3.1	11
82	Single-step scalable conversion of waste natural oils to carbon nanowhiskers and their interaction with mammalian cells. Journal of Nanoparticle Research, 2013, 15, 1.	1.9	11
83	Pd nanoparticle concentration dependent self-assembly of Pd@SiO2 nanoparticles into leaching resistant microcubes. Chemical Communications, 2014, 50, 10510-10512.	4.1	11
84	Charge Transport between Coaxial Polymer Nanorods and Grafted All-Inorganic Perovskite Nanocrystals for Hybrid Organic Solar Cells with Enhanced Photoconversion Efficiency. Journal of Physical Chemistry C, 2020, 124, 246-255.	3.1	11
85	Unraveling the Charge Transport Mechanism in Mechanochemically Processed Hybrid Perovskite Solar Cell. Langmuir, 2021, 37, 5513-5521.	3.5	11
86	Exchange Bias and Spin-Glass-Like Ordering inε-Fe3N–CrN Nanocomposites. Japanese Journal of Applied Physics, 2007, 46, 980-987.	1.5	10
87	Synthesis, Characterization and Magnetic Interactions Study of ε-Fe3N–CrN Nanorods. Journal of Nanoscience and Nanotechnology, 2007, 7, 1836-1840.	0.9	10
88	Coexistence of High Magnetization and Anisotropy with Non-monotonic Particle Size Effect in Ferromagnetic PrMnO ₃ Nanoparticles. Journal of Physical Chemistry C, 2017, 121, 21029-21036.	3.1	10
89	When multiferroics become photoelectrochemical catalysts: A case study with BiFeO3/La2NiMnO6. Materials Chemistry and Physics, 2020, 244, 122685.	4.0	10

90Synthesis and structural investigation of É>-Fe3â^'xNixN (0.0≠kâ‰0.8) nanoparticles. Progress in Crystal
Growth and Characterization of Materials, 2006, 52, 132-141.4.09

SAYAN BHATTACHARYYA

#	Article	IF	CITATIONS
91	Observation of exchange bias and spin-glass-like ordering in É>-Fe2.8Cr0.2N nanoparticles. Pramana - Journal of Physics, 2008, 70, 367-373.	1.8	9
92	Surfactant-Mediated Resistance to Surface Oxidation in MnO Nanostructures. ACS Omega, 2017, 2, 3028-3035.	3.5	9
93	Bimetallic Zero-Valent Alloy with Measured High-Valent Surface States to Reinforce the Bifunctional Activity in Rechargeable Zinc-Air Batteries. ACS Sustainable Chemistry and Engineering, 2021, 9, 14868-14880.	6.7	9
94	Cs ₃ Bi ₂ I ₉ nanodiscs with phase and Bi(<scp>iii</scp>) state stability under reductive potential or illumination for H ₂ generation from diluted aqueous HI. Nanoscale, 2022, 14, 4281-4291.	5.6	9
95	The Perfect Imperfections in Electrocatalysts. Chemical Record, 2022, 22, .	5.8	9
96	Investigation of γ′-Fe4Nâ^'GaN Nanocomposites: Structural and Magnetic Characterization, Mössbauer Spectroscopy and Ab Initio Calculations. Journal of Physical Chemistry C, 2010, 114, 17542-17549.	3.1	8
97	Advanced Nanoporous Materials: Synthesis, Properties, and Applications. Journal of Nanomaterials, 2014, 2014, 1-2.	2.7	8
98	Pressure-induced emission enhancement and bandgap narrowing: Experimental investigations and first-principles theoretical simulations on the model halide perovskite <mml:math xmlns:mml="http://www.w3.org/1998/Math/MathML"> <mml:msub> <mml:mrow> <mml:mi>Cs</mml:mi> Physical Review B, 2022, 105, .</mml:mrow></mml:msub></mml:math>	ırö w > <mr< td=""><td>nl<mark>8</mark>mn>3</td></mr<>	nl <mark>8</mark> mn>3
99	Magnetic properties ofÉ>Fe3-xNixN nanoparticles. Physica Status Solidi C: Current Topics in Solid State Physics, 2004, 1, 3764-3768.	0.8	7
100	Mössbauer studies of É›-Fe3â^'x Ni x N and γ′-Fe4â^'y Ni y N nanoparticles. Hyperfine Interactions, 2007, 165, 147-151.	0.5	7
101	Comprehensive and Highâ€throughput Electrolysis of Water and Urea by 3–5 nm Nickel and Copper Coordination Polymers. Chemistry - an Asian Journal, 2021, 16, 3444-3452.	3.3	7
102	Magnetic properties of Cd _{1 â^'<i>x</i>} Mn _{<i>x</i>} Te/C nanocrystals. Nanotechnology, 2011, 22, 075703.	2.6	6
103	The destructive spontaneous ingression of tunable silica nanosheets through cancer cell membranes. Chemical Science, 2019, 10, 6184-6192.	7.4	6
104	Tweaking Nickel with Minimal Silver in a Heterogeneous Alloy of Decahedral Geometry to Deliver Platinumâ€like Hydrogen Evolution Activity. Angewandte Chemie, 2020, 132, 2903-2911.	2.0	6
105	Direct Correlation of the Morphologies of Metal Carbonates, Oxycarbonates, and Oxides Synthesized by Dry Autoclaving to the Intrinsic Properties of the Metals. Crystal Growth and Design, 2014, 14, 4060-4067.	3.0	5
106	Thermal Nonlinear Refraction in Cesium Lead Halide Perovskite Nanostructure Colloids. Journal of Physical Chemistry C, 2020, 124, 15558-15564.	3.1	5
107	Extensive Parallelism between Crystal Parameters and Magnetic Phase Transitions of Unusually Ferromagnetic Praseodymium Manganite Nanoparticles. Inorganic Chemistry, 2016, 55, 7903-7911.	4.0	4
108	An unconventional route to an ambipolar azaheterocycle and its <i>in situ</i> generated radical anion. Organic and Biomolecular Chemistry, 2021, 19, 5114-5120.	2.8	4

#	Article	IF	CITATIONS
109	A Fragmentizing Interface to a Large Corpus of Digitized Text: (Post)humanism and Non-consumptive Reading via Features. Interdisciplinary Science Reviews, 2015, 40, 61-77.	1.4	3
110	Carrier relaxation dynamics of ZnxCd1â^'xSe/C core/shell nanocrystals with phase separation as studied by time-resolved cathodoluminescence. Applied Physics Letters, 2009, 95, 181903.	3.3	2
111	Charge Transfer and Ultrafast Nonlinear Optical Properties above Percolation Threshold in Graphene-Induced ZnTTBPc. Journal of Physical Chemistry C, 2020, 124, 7039-7047.	3.1	2
112	Optical and Structural Studies of Phase Separation in Zn[sub x]Cd[sub 1â^'x]Seâ^•C Coreâ^•Shell Nanocrystals. , 2011, , .		1
113	Hot Phonon and Auger Heating Mediated Slow Intraband Carrier Relaxation in Mixed Halide Perovskite. IEEE Journal of Quantum Electronics, 2020, , 1-1.	1.9	1
114	Phase-separation in ZnxCd1-xSe/C Core/shell nanocrystals studied with cathodoluminescence spectroscopy. Materials Research Society Symposia Proceedings, 2010, 1260, 1.	0.1	0